

1. Question 1

- (1.1) The open-loop step response of the system is shown in the Simulink model (Figure 1) below with the response shown in Figure 2.

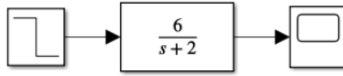


Figure 1: Simulink model of the open-loop step response

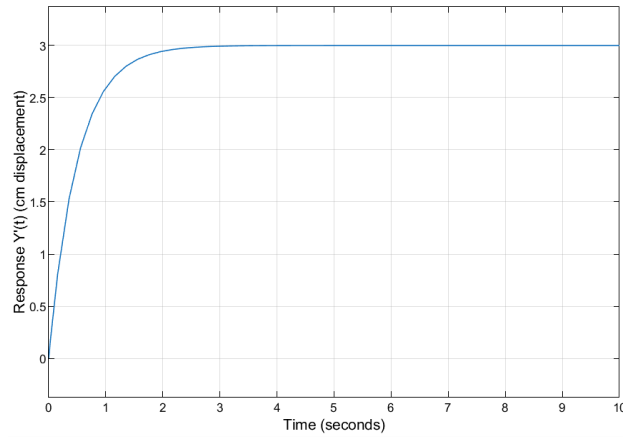


Figure 2: Open-loop step response

To identify the gain and time constant for this system, we can rearrange the transfer function to isolate the gain K and time constant τ :

The given transfer function is:

$$G_p(s) = \frac{6}{s+2}$$

To express this in the standard first-order form, which is:

$$G(s) = \frac{K}{\tau s + 1}$$

where K is the gain and τ is the time constant.

We rearrange $G_p(s)$ as follows:

$$G_p(s) = \frac{6}{2(\frac{1}{2}s + 1)} = \frac{3}{\frac{1}{2}s + 1}$$

Thus, we identify the gain K and the time constant τ as:

$$K = 3, \quad \tau = \frac{1}{2}$$

- (1.2) The closed-loop feedback control with a proportional controller is shown below in Figure 3. The transfer function $G_c(s)$ can also be represented by a proportional gain K_c .

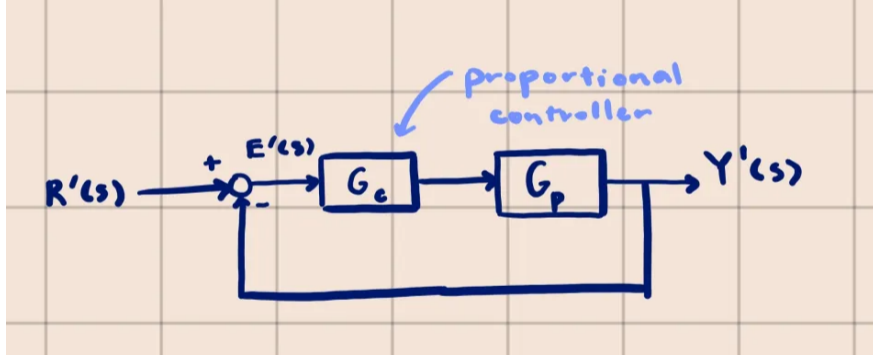


Figure 3: Simulink model of the closed-loop feedback control with a proportional controller

- (1.3) The Simulink model is shown below in Figure 4. The response of the system is shown in Figure 5.



Figure 4: Simulink model of the closed-loop feedback control with a proportional controller

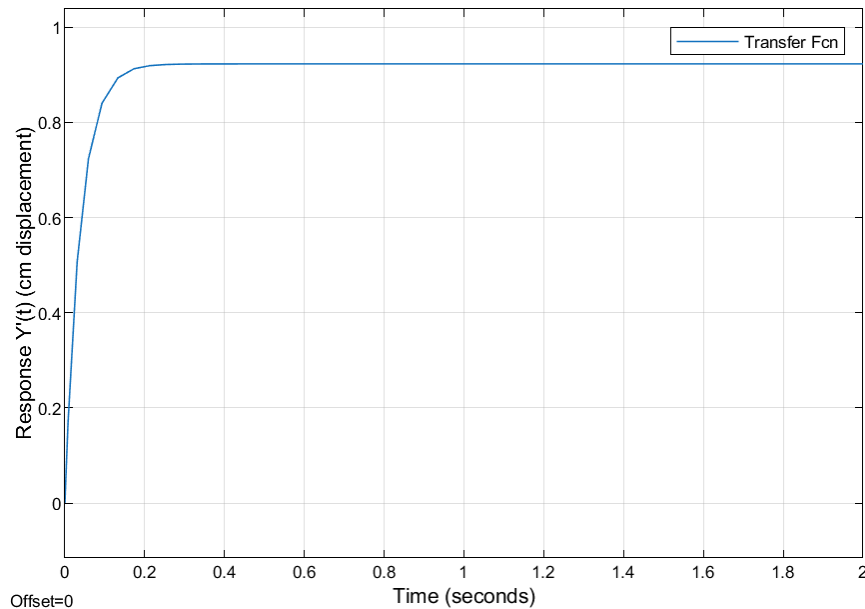


Figure 5: Closed-loop step response

(1.4) The closed-loop transfer function $T(s)$ is given by:

$$T(s) = \frac{Y'(s)}{R'(s)} = \frac{G_c(s)G_p(s)}{1 + G_c(s)G_p(s)}$$

Where $G_c(s) = K_c = 4$ (proportional controller) and $G_p(s) = \frac{6}{s+2}$ (plant transfer function). Substituting the transfer functions:

$$T(s) = \frac{4 \cdot \frac{6}{s+2}}{1 + 4 \cdot \frac{6}{s+2}}$$

Simplifying:

$$T(s) = \frac{\frac{24}{s+2}}{1 + \frac{24}{s+2}} = \frac{24}{s + 2 + 24} = \frac{24}{s + 26}$$

Thus, the closed-loop transfer function is:

$$T(s) = \frac{24}{s + 26}$$

We then apply the Final Value Theorem, which states that:

$$\lim_{t \rightarrow \infty} y(t) = \lim_{s \rightarrow 0} sY(s)$$

For a unit step input $R'(s) = \frac{1}{s}$, the Laplace transform of the output is:

$$Y'(s) = T(s)R'(s) = \frac{24}{s + 26} \cdot \frac{1}{s}$$

Applying the FVT:

$$\lim_{t \rightarrow \infty} y(t) = \lim_{s \rightarrow 0} s \cdot \frac{24}{(s + 26)s} = \lim_{s \rightarrow 0} \frac{24}{s + 26} = \frac{24}{26} = \frac{12}{13} \approx 0.923$$

Putting this into the offset equation, we get the following offset:

$$\text{Offset} = \lim_{t \rightarrow \infty} r(t) - \lim_{t \rightarrow \infty} y(t) = 1 - 0.923 = 0.077$$

The steady-state value of the output is approximately 0.923. Since the system is operating on displacement from a rack assembly with a step input, the set point is 1. Thus, the offset of this system is approximately 0.077. This can be confirmed by referring to the step response in Figure 5, where we can see the offset is approximately 0.077.

- (1.5) The closed-loop system for controller gains $K_c = 0.25, 1, 2, 4, 10$ are shown in Figure 6. Observing the results, we can see that the offset of the system decreases as the proportional gain increases. This is because the higher the proportional gain, the more the controller can correct for the error, leading to a smaller offset – it essentially gets more aggressive and faster than higher K_c .

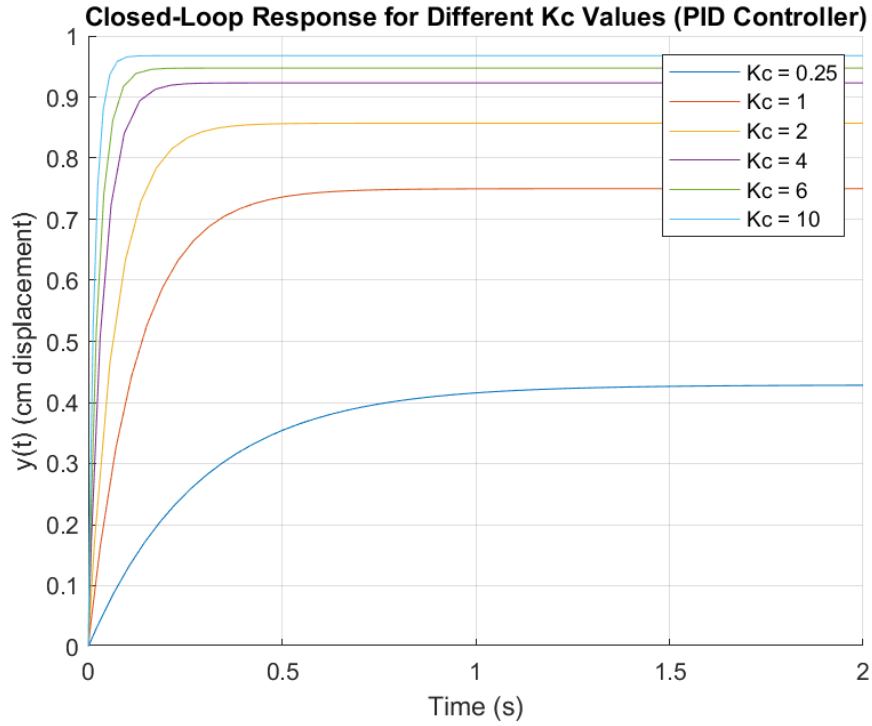


Figure 6: Closed-loop step response for different controller gains

- (1.6) We want to find the controller gain K_c such that the offset is less than 0.08. The offset is given by:

$$\text{Offset} = \lim_{t \rightarrow \infty} (r(t) - y(t))$$

Using the Final Value Theorem:

$$\text{Offset} = \lim_{s \rightarrow 0} \left(1 - \frac{K_c \cdot G_p}{1 + K_c \cdot G_p} \right)$$

With $G_p = \frac{6}{s+2}$, we evaluate at $s = 0$:

$$\text{Offset} = 1 - \frac{K_c \cdot \frac{6}{0+2}}{1 + K_c \cdot \frac{6}{0+2}} = 1 - \frac{3K_c}{1 + 3K_c}$$

We require that the offset be less than 0.08:

$$0.08 > 1 - \frac{3K_c}{1 + 3K_c}$$

Rearranging the inequality:

$$\frac{3K_c}{1 + 3K_c} > 1 - 0.08 = 0.92$$

$$3K_c > 0.92(1 + 3K_c)$$

$$K_c > 3.8333...$$

Therefore, the controller gain K_c must be greater than approximately 3.83 to achieve an offset less than 0.08.

- (1.7) We change from the proportional controller to the proportional-integral controller by adjusting the transfer function $G_c(s)$ to include an integral term. The transfer function for the PI controller is given by:

$$G_c(s) = K_c \left(1 + \frac{1}{\tau_I s} \right)$$

Where $K_c = 3$ and $\tau_I = 0.05$. The response of the system is shown in Figure 7.

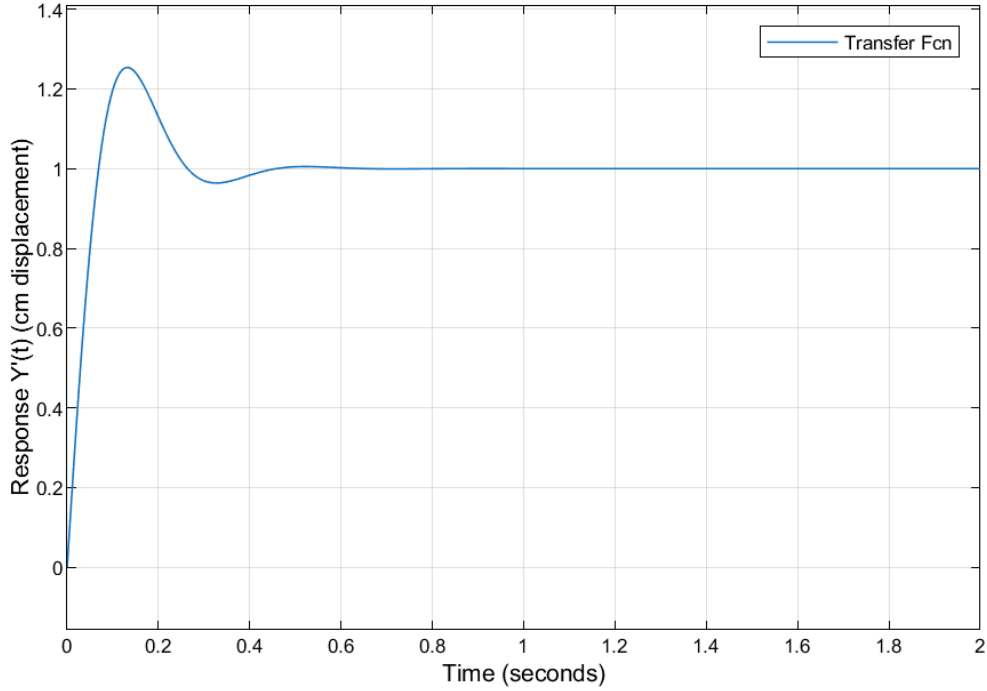


Figure 7: Closed-loop step response with a PI controller

- (1.8) Given the below two transfer functions in our system:

$$G_c = K_c \left(1 + \frac{1}{\tau_I s} \right)$$

$$G_p = \frac{6}{s + 2} = \frac{K_p}{\tau_p s + 1}$$

where,

$$K_p = 3, \quad \tau_p = \frac{1}{2}, \quad K_c = 3, \quad \tau_I = 0.05$$

Together, the closed-loop transfer function for the system becomes:

$$\frac{Y'(s)}{R'(s)} = \frac{\tau_I s + 1}{\frac{\tau_I \tau_p}{K_c K_p} s^2 + \tau_I \frac{(1+K_c K_p)}{K_c K_p} s + 1}$$

We can use the equations as presented in the lecture to calculate the time constant τ and the damping factor ζ .

$$\tau = \sqrt{\frac{\tau_I \tau_p}{K_c K_p}} = \sqrt{\frac{(0.05)(\frac{1}{2})}{(3)(3)}} = \sqrt{0.00278}$$

$$\tau \approx 0.0527$$

$$\zeta = \frac{1}{2}(1 + K_c K_p) \sqrt{\frac{\tau_I}{K_c K_p \tau_p}} = \frac{1}{2}(1 + 9) \sqrt{\frac{0.05}{(3)(3)(\frac{1}{2})}}$$

$$\zeta \approx 0.526$$

We also derive the closed-loop gain K .

$$K = \tau_I s + 1 = 0.05s + 1$$

At steady state, s becomes 0 due to the FVT. Thus, $K(0) = 1$, which confirms that the system should track a step input without steady-state error. This is expected of a system with a PI-Controller – there should be no offset.

The calculated time constant is approximately $\tau \approx 0.0527$, which suggests the system should settle relatively quickly. The expected settling time, approximately $5\tau = 0.2635s$, can be seen in Figure 7, where it settles around that point.

The damping factor was found to be $\zeta \approx 0.526$, suggesting a slightly underdamped response. This means the system should exhibit small oscillations but should not overshoot excessively, as observed in the above figure.

- (1.9) The closed-loop system for integral times $\tau_I = 0.01, 0.05, 0.1, 0.5, 1, 2$ are shown in Figure 8. As the integral time decreases, the system has an increased speed of response but also a higher relative overshoot.

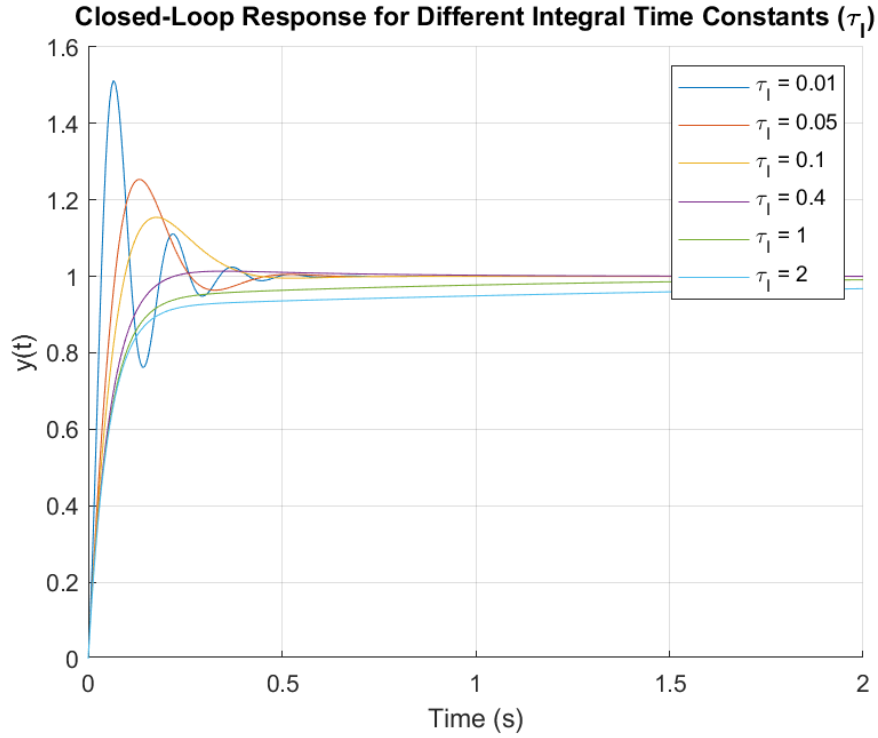


Figure 8: Closed-loop step response for different integral times

From comparing the different integral time constants, we can see that τ_I dictates in a PI controller the trade-off between response speed and stability. Small values (e.g., $\tau_I = 0.01$) yield fast responses but can cause excessive overshoot and oscillations. Larger values (e.g., $\tau_I = 2$) improve stability with less overshoot but result in slower responses. Tuning τ_I aims to find an optimal value, like $\tau_I = 0.4$, that balances speed and stability according to the specific process requirements. This is due to the mathematical relationship between τ_I and the damping factor and time constant, which affect the system's response characteristics.

- (1.10) The surface plots are shown below in Figure 9 and Figure 10. The surface plots show the relationship between the integral time constant τ_I and the damping factor ζ with the settling time and the relative overshoot.

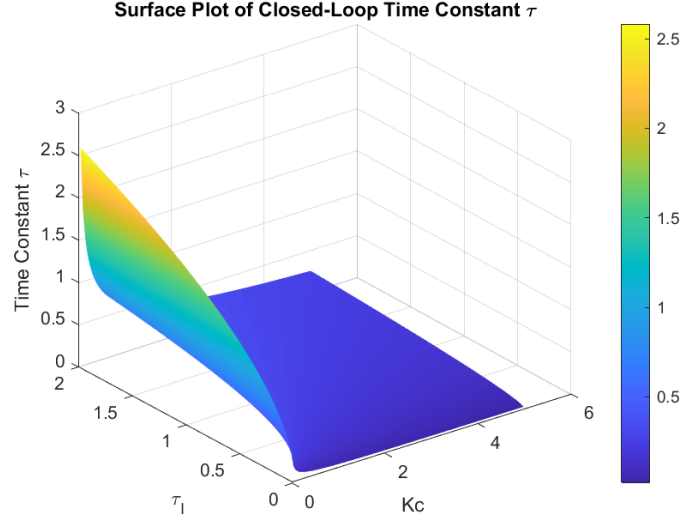


Figure 9: Surface plot of settling time and integral time constant

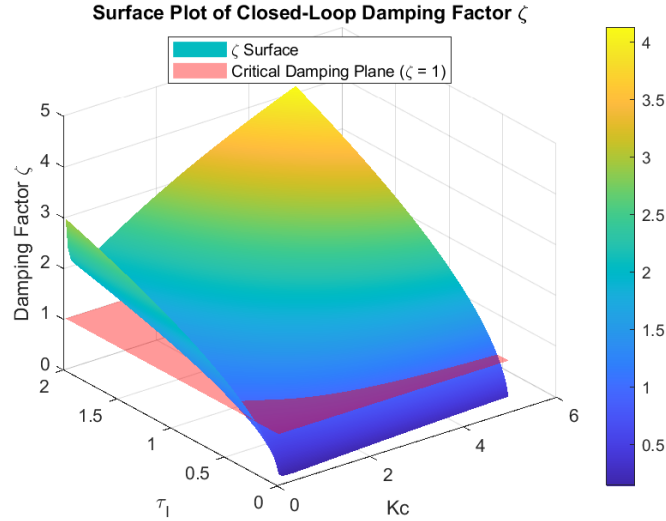


Figure 10: Surface plot of relative overshoot and integral time constant

The surface plots for the closed-loop time constant (τ) and damping factor (ζ) reveal important insights into the system's dynamics and the trade-offs between speed and stability. The time constant plot shows that τ decreases as the proportional gain (K_c) increases, indicating a faster system response. However, very high K_c values can lead to instability, as seen in the damping factor plot, where higher K_c 's tend to increase the damping factor past a magnitude of 1. Similarly, smaller integral time constants (τ_I) reduce τ , but overly small τ_I can destabilize

the system. The goal is to minimize τ for a fast response while ensuring the system remains stable.

The damping factor plot highlights that a value of ζ close to 1 is ideal, as it represents critical damping, where the system responds quickly without oscillations. For small K_c , the system is underdamped ($\zeta < 1$), leading to oscillations, while very large K_c results in overdamping ($\zeta > 1$), causing a sluggish response. Larger τ_I values increase ζ , while smaller τ_I reduce it, potentially leading to instability.

To optimize the system, we aim to balance speed and stability by selecting K_c and τ_I values that minimize τ while keeping ζ close to 1. From the plots, moderate K_c values (e.g., 2–4) and small-to-moderate τ_I values (e.g., 0.2–0.5) are likely to achieve this balance, providing a fast and stable response.

- (1.11) The curve that represents the intersection between the surface $\zeta = f(K_c, \tau_I)$ and plane $\zeta = 1$. The curve is shown in Figure 11.

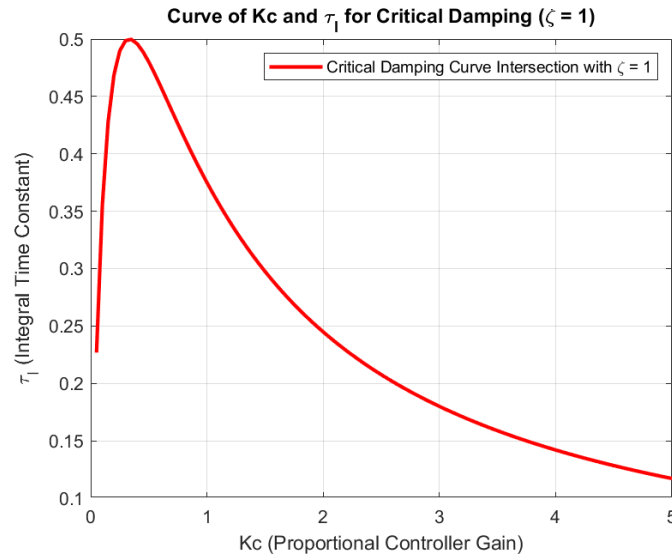


Figure 11: Intersection curve between the surface and plane

- (1.12) To optimize the system, we want to choose parameters that also have the lowest closed-loop time constant, as well as having a damping factor of 1. The closed-loop time constant is thus overlayed over the Figure 11 in Figure 12.

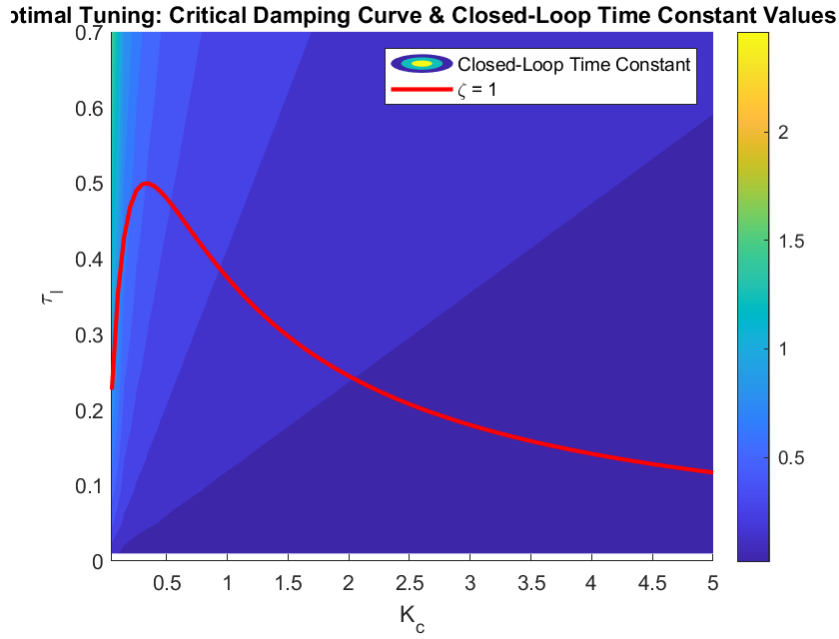


Figure 12: Intersection curve between the surface and plane with the closed-loop time constant

Given the constraint that $K_c \leq 5$, the optimal values that follows the rational above occurs in Figure 12 at $K_c = 5$ and $\tau_I = 0.117187$. This point represents the optimal balance between speed and stability, ensuring a fast response without oscillations.

- (1.13) Graphing the above optimal tuning parameters, we get the following results for yt . It exhibits the system characteristics that we were optimizing for in thh previous questions – we have the quickest response that could occur while critically damped, as shown in Figure 13. Putting the system into ideal form, we get the below:

$$G_c(s) = 5 \left(1 + \frac{1}{0.117187s} \right)$$

Turning this into parallel form gives us the following:

$$G_c(s) = 5 + \frac{5}{0.117187} \frac{1}{s}$$

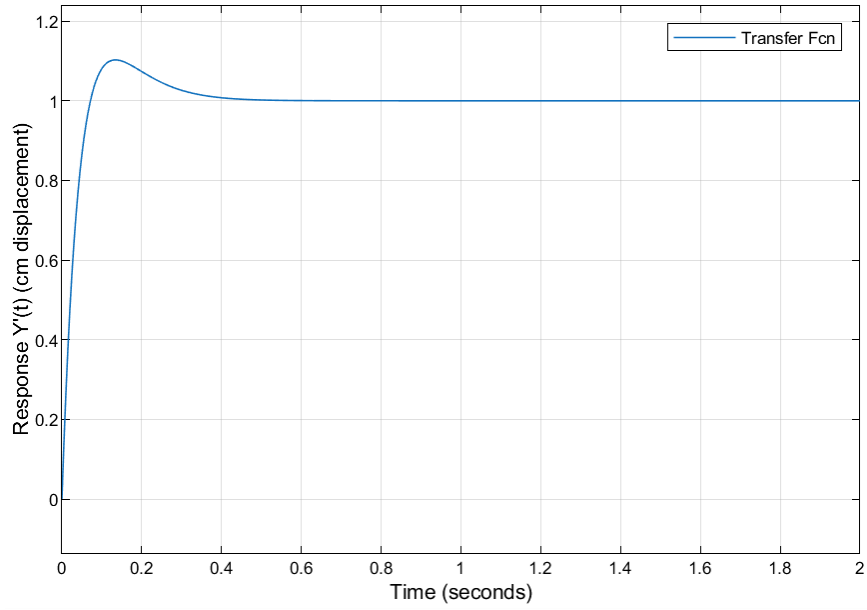


Figure 13: System response with optimal tuning parameters

- (1.14) With the newly added sensor, we get the following result with our previously optimized system in Figure 14 from the model shown in Figure 15. Compared to the ideal scenario where there was no sensor dynamics (Figure 13), the system now has more oscillations. This is due to the sensor dynamics introducing a delay in the feedback loop, causing the system to overshoot and oscillate before stabilizing.

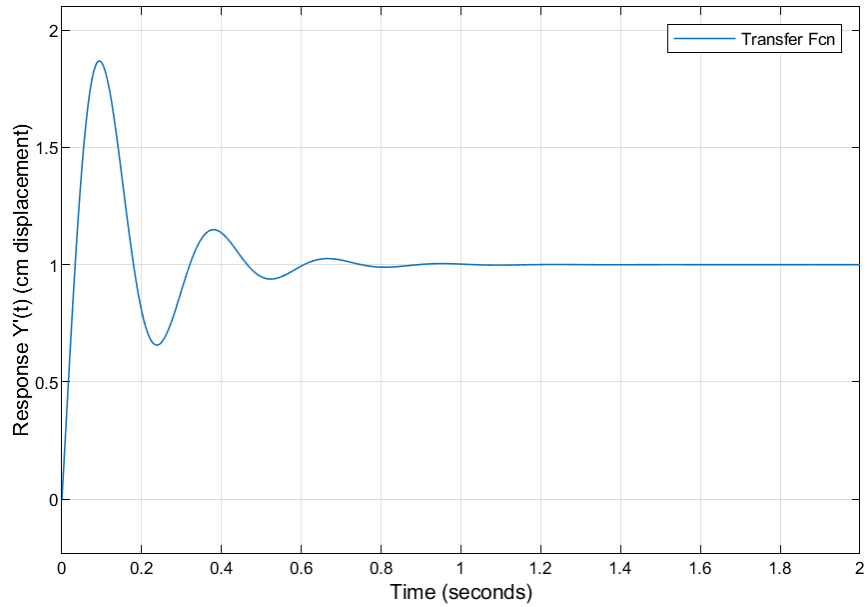


Figure 14: System response with sensor dynamics

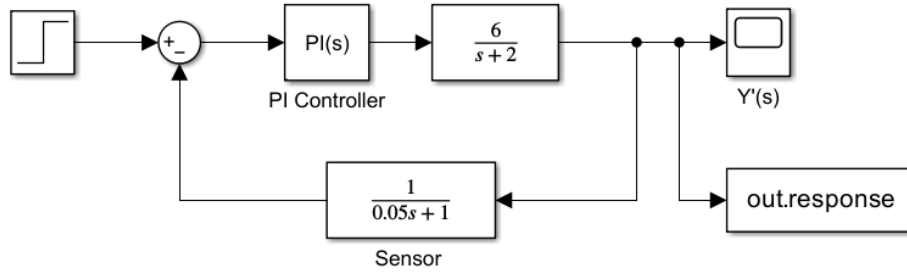


Figure 15: Simulink model of the system with sensor dynamics

These are no longer the most optimal tuning parameters for this system. We need to reduce the oscillations while still keeping the time constant low. As we learned from lecture, we can achieve less of an overshoot by decreasing K_c or increasing τ_I . We can change these parameters independently of each other at each tuning iteration to isolate their effects on the system. We can then observe the system's response and adjust the parameters accordingly to achieve the desired response.

Initially, we decreased the K_c value from 5 to 3, this reduced the overshoot by a bit but not too much. We then incremented the τ_I to 0.4, which decreased the overshoot even more. K_c was then reduced to just 1, where we saw minimal overshoot, however this new overshoot caused the settling time to be prolonged. To fix this, we went through one bonus tuning iteration increasing the τ_I to reduce overshoot. Overall, the best tuning parameters ended up being $K_c = 1$ and $\tau_I = 0.5$. As expected, these final tuning parameters involved decreasing K_c and increasing τ_I .

All three + one iterations plus the original response is shown below in Figure 16.

Closed-Loop Response with Sensor Dynamics for Different Tuning Iterations

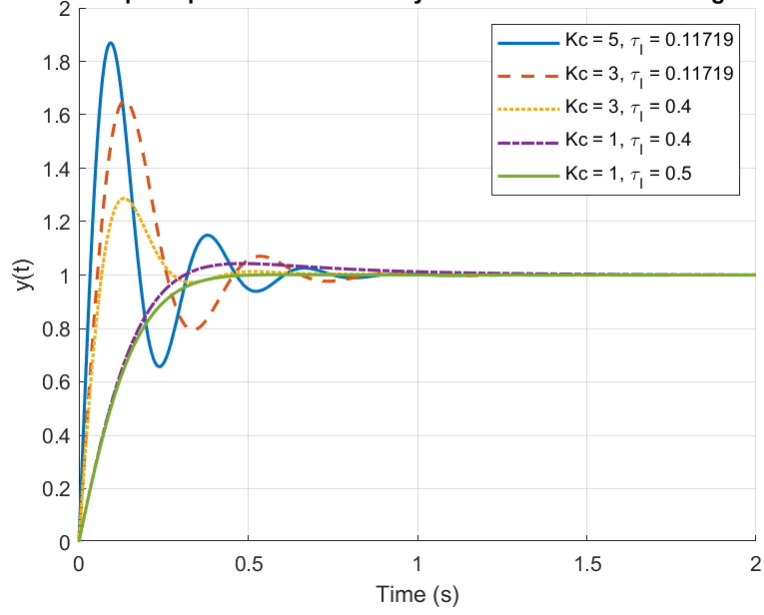


Figure 16: System response with sensor dynamics and different K_c values

2. Question 2

- (2.1) To assess the stability of the open-loop system, we examined the poles of the system's transfer functions derived from laplacing (true verb) the linearized model. (Figure 17) shows the TFs for the system found from A2 solutions doc:

Question 2

$$\begin{aligned}
 2.1 \quad C_A'(s) &= \underbrace{\frac{B}{(s-\alpha)}}_{G_1(s)} T'(s) + \underbrace{\frac{\gamma}{(s-\alpha)}}_{G_2(s)} C_{Ao}'(s) & \alpha &= -\frac{F}{V} - K_0 e^{-\frac{E}{RT}} \\
 T'(s) &= \underbrace{\frac{\delta}{(s-\epsilon)}}_{G_3(s)} C_A'(s) + \underbrace{\frac{\eta}{(s-\epsilon)}}_{G_4(s)} Q'(s) & B &= -\frac{EK_0\bar{C}_A}{RT^2} e^{-\frac{E}{RT}} \\
 & & \gamma &= \frac{F}{V} \\
 & & \delta &= -\frac{\Delta HK_0}{\rho C_p} e^{-\frac{E}{RT}} \\
 & & \epsilon &= -\frac{F}{V} - \frac{K_0\bar{C}_A\Delta HE}{\rho C_p RT^2} e^{-\frac{E}{RT}} \\
 & & \eta &= \frac{1}{\rho C_p V}
 \end{aligned}$$

Figure 17: Transfer functions for the system.

The relevant transfer functions, based on the deviation variables, are:

$$G_1(s) = \frac{\beta}{s - \alpha}, \quad G_2(s) = \frac{\gamma}{s - \alpha}, \quad G_3(s) = \frac{\delta}{s - \epsilon}, \quad G_4(s) = \frac{\eta}{s - \epsilon}$$

Using MATLAB and the given reactor parameters, the following values were computed:

$$\begin{aligned}
 \alpha &= -13.606483 \\
 \beta &= -0.013089 \\
 \gamma &= 0.400000 \\
 \delta &= 1918.753467 \\
 \epsilon &= 1.501699 \\
 \eta &= 0.006079
 \end{aligned}$$

This gives us the following pole locations:

- Poles of $G_1(s)$ and $G_2(s)$: $s = -13.606483$
- Poles of $G_3(s)$ and $G_4(s)$: $s = 1.501699$

Since the poles of $G_3(s) = \frac{T'(s)}{C_A'(s)}$ and $G_4(s) = \frac{Q'(s)}{T'(s)}$ both have positive real parts, the temperature deviation $T'(s)$ exhibits an unstable response in open-loop. Furthermore, from the structure of the system, the state $T'(s)$ is an input into $G_1(s)$, which feeds into $C_A'(s)$. Thus, instability in $T'(s)$ directly destabilizes $C_A'(s)$ as well. Thus it is an unstable open-loop system.

(2.2) Using the TFs found in 2.1 (see Figure 17), we computed the math below to find and build the block diagram (Figure 18).

$$2.2 \quad C_A'(s) = G_1(s)T'(s) + G_2(s)C_{A0}'(s)$$

$$T'(s) = G_3(s)C_A'(s) + G_4(s)Q'(s)$$

dropping (s) for future math bc lazy

$$C_A' = G_1(G_3C_A' + G_4Q') + G_2C_{A0}'$$

$$C_A' = G_1G_3C_A' + G_1G_4Q' + G_2C_{A0}'$$

$$C_A'(1 - G_1G_3) = G_1G_4Q' + G_2C_{A0}'$$

$$C_A' = \frac{G_1G_4}{1 - G_1G_3} Q' + \frac{G_2}{1 - G_1G_3} C_{A0}'$$

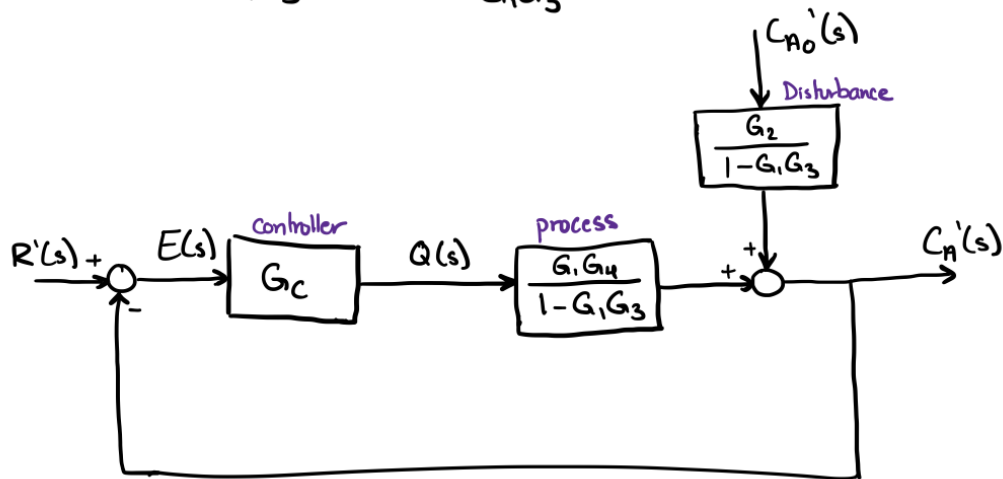


Figure 18: Derivation of block diagram where $C_A'(s)$ is the output, $C_{A0}'(s)$ is the disturbance, and $Q'(s)$ is the input determined by the controller.

- (2.3) From the derived closed-loop block diagram in Figure 18, the open-loop transfer function from the heat input $Q'(s)$ to the outlet concentration $C'_A(s)$ is:

$$\frac{C'_A(s)}{Q'(s)} = \frac{G_1(s)G_4(s)}{1 - G_1(s)G_3(s)}$$

We use the previously computed parameter values from Matlab to see what the gain will be by inspection:

$$\begin{aligned}\beta = -0.013089 & \Rightarrow G_1(s) = \frac{\beta}{s - \alpha} \\ \delta = 1918.753467 & \Rightarrow G_3(s) = \frac{\delta}{s - \epsilon} \\ \eta = 0.006079 & \Rightarrow G_4(s) = \frac{\eta}{s - \epsilon}\end{aligned}$$

Sign of the Numerator G_1G_4

$$\beta < 0, \quad \eta > 0 \quad \Rightarrow \quad G_1G_4 < 0$$

Sign of the Denominator $1 - G_1G_3$

$$\beta < 0, \quad \delta > 0 \quad \Rightarrow \quad G_1G_3 < 0 \quad \Rightarrow \quad 1 - G_1G_3 > 1$$

Thus:

$$\frac{C'_A(s)}{Q'(s)} = \frac{\text{negative}}{\text{positive}} = \text{negative}$$

The process gain from $Q'(s)$ to $C'_A(s)$ is clearly negative based on the math. This implies that increasing the heat input results in a decrease in the outlet concentration C'_A , which makes sense with the exothermic nature of the reaction — increasing heat raises temperature, which increases reaction rate, therefore consuming more of A . Also using Matlab's `dcgain` function, we found the gain would be -0.000017, which helps us double check that the gain is negative.

- (2.4) From the previous analysis in question 2.3, we found that the TF from the manipulated input $Q'(s)$ to the controlled output $C'_A(s)$ has a negative gain. In the feedback control system, the controller output is based on the error signal $E(s) = R'(s) - C'_A(s)$, and the controller applies a gain K_C to compute the input to the process:

$$Q'(s) = G_C(s)E(s) = K_C E(s)$$

If the sign of K_C does not match the sign of the process gain, the feedback becomes positive feedback rather than negative feedback since the input $Q'(s)$ will be proportional to the error, and continuously move the output away from setpoint, which leads to instability. This was also mentioned in class that controller gain and process gain should be the same sign. Thus, K_C should be negative.

We can also assess the block diagram. If $C'_A(s)$ goes above setpoint, we get that $E(s) = R'(s) - C'_A(s) < 0$. With the negative error, we want to increase heat

(positive $Q'(s)$), since as mentioned in question 2.3, increasing temperature will use up more of A , reducing $C'_A(s)$. To get a positive $Q'(s)$ in this test case, the K_C must be negative.

- (2.5) To design the PI controller to reject disturbances and keep the outlet concentration as close to zero as possible, we simulated the closed-loop system for several values of K_c and τ_I , using the transfer functions derived analytically. These transfer functions, derived from the linearized system equations, are shown in Figures 19 and 20.

$$\begin{aligned}
 \frac{C'_A}{Q'} &= \frac{G_1 G_4}{1 - G_1 G_3} \\
 &= \frac{\frac{B\eta}{(s-\alpha)(s-\epsilon)}}{1 - \frac{B\delta}{(s-\alpha)(s-\epsilon)}} \\
 &= \frac{B\eta}{(s-\alpha)(s-\epsilon) - B\delta} \\
 &= \frac{B\eta}{s^2 - (\alpha + \epsilon)s + \alpha\epsilon - B\delta} \\
 &= \frac{-7.956803 \times 10^{-5}}{s^2 + 12.104784s + 4.681722}
 \end{aligned}
 \quad
 \begin{aligned}
 \frac{C'_A}{C'_{A0}} &= \frac{G_2}{1 - G_1 G_3} \\
 &= \frac{\frac{\gamma}{s-\alpha}}{1 - \frac{B\delta}{(s-\alpha)(s-\epsilon)}} \\
 &= \frac{\gamma(s-\epsilon)}{(s-\alpha)(s-\epsilon) - B\delta} \\
 &= \frac{\gamma s - \gamma\epsilon}{s^2 - (\alpha + \epsilon)s + \alpha\epsilon - B\delta} \\
 &= \frac{0.4s - 0.600680}{s^2 + 12.104784s + 4.681722}
 \end{aligned}$$

← plug values →

Figure 19: Transfer function derivations for C'_A/Q' and C'_A/C'_{A0}

$$T' = G_3(G_1 T' + G_2 C_{A0}') + G_4 Q'$$

$$T' = G_3 G_1 T' + G_3 G_2 C_{A0}' + G_4 Q'$$

$$T'(1 - G_3 G_1) = G_3 G_2 C_{A0}' + G_4 Q'$$

$$\frac{T'}{C_{A0}'} = \frac{G_3 G_2}{1 - G_3 G_1}$$

$$= \frac{\frac{8\gamma}{(s-\epsilon)(s-\alpha)}}{1 - \frac{8\beta}{(s-\epsilon)(s-\alpha)}}$$

$$= \frac{8\gamma}{s^2 - (\alpha + \epsilon)s + \alpha\epsilon - 8\beta}$$

$$= \frac{767.501387}{s^2 + 12.104784s + 4.681722}$$

$$\frac{T'}{Q'} = \frac{G_4}{1 - G_3 G_1}$$

$$= \frac{\frac{\eta}{(s-\epsilon)}}{1 - \frac{8\beta}{(s-\alpha)(s-\epsilon)}}$$

$$= \frac{\eta s - \eta\alpha}{s^2 - (\alpha + \epsilon)s + \alpha\epsilon - 8\beta}$$

$$= \frac{0.006076s + 0.082714}{s^2 + 12.104784s + 4.681722}$$

Figure 20: Transfer function derivations for T'/C'_{A0} and T'/Q'

The design goal is to ensure the system meets the following specifications:

- $Q'(t) \geq -2000$ kJ/min
- $T'(t) \leq 15$ K (Note K vs C doesn't matter since it's deviation which are equal)
- $|C'_A(t)| \leq 0.01$ kmol/m³
- All outputs return close to zero within 40 minutes

We evaluated four controller configurations:

Test Case 1: $K_c = -1.00$, $\tau_I = 1.00$

This test case acts as the baseline, shown in Figure 21. As expected, the system is too sluggish. The concentration $C'_A(t)$ drifts below -0.01 kmol/m³ and does not return to the setpoint by 40 minutes. Additionally, the temperature $T'(t)$ exceeds the safety threshold of 15 K. The control effort $Q'(t)$ remains within bounds, but the error $E'(t)$ continues to increase and plateaus, indicating poor control. To improve performance, we decided to try increasing the aggressiveness of the controller by scaling K_c up by a factor of 100.

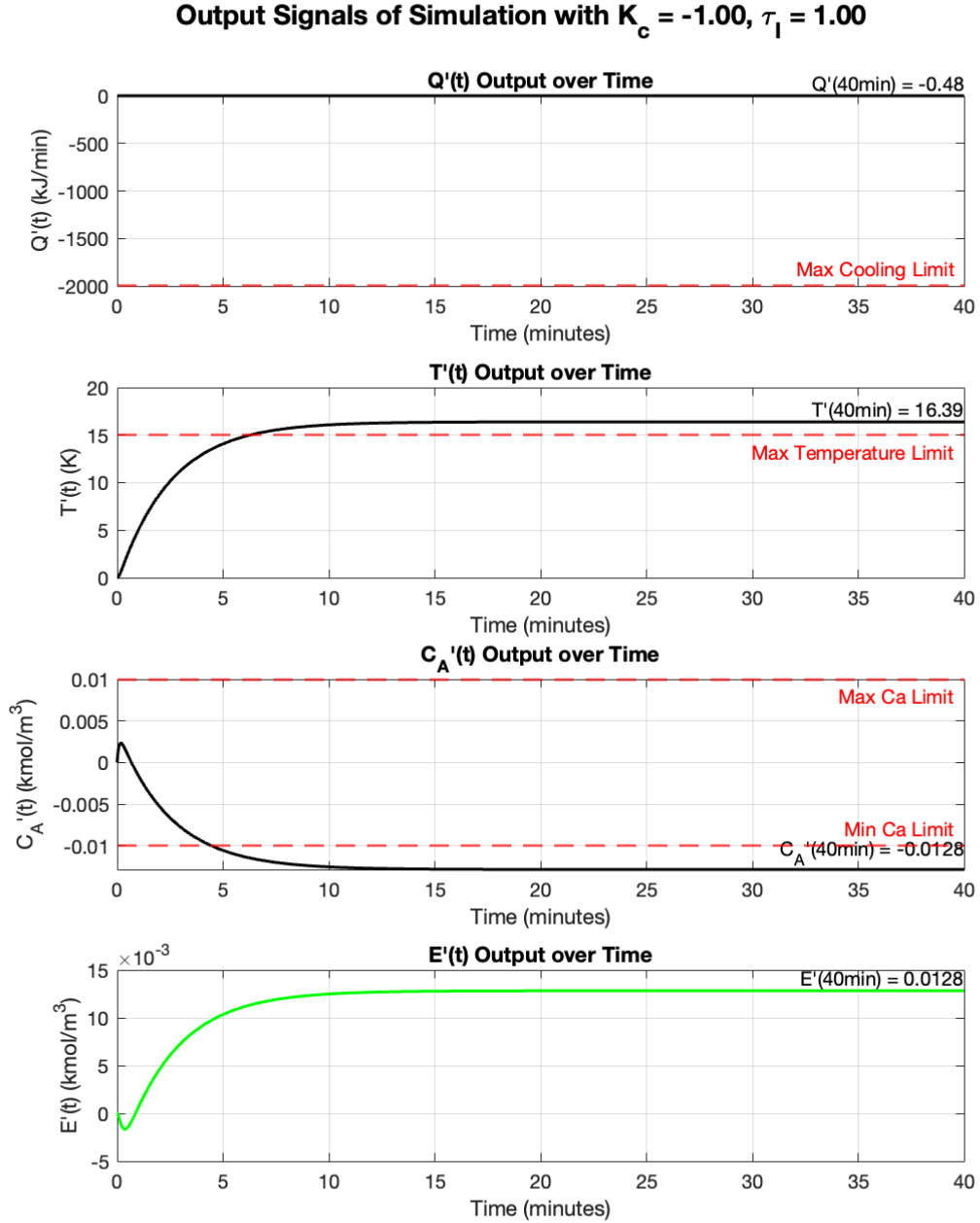


Figure 21: System response with $K_c = -1.00$, $\tau_I = 1.00$

Test Case 2: $K_c = -100.00$, $\tau_I = 1.00$

Shown in Figure 22, this test case improves the response slightly. We observe that $C'_A(t)$ begins to return toward the setpoint, though it still does not settle within bounds by 40 minutes. Temperature $T'(t)$ is closer to the limit but still slightly exceeds 15 K. This suggests the controller needs to act faster. Since reducing τ_I increases responsiveness, the next step we decided to try was to decrease τ_I .

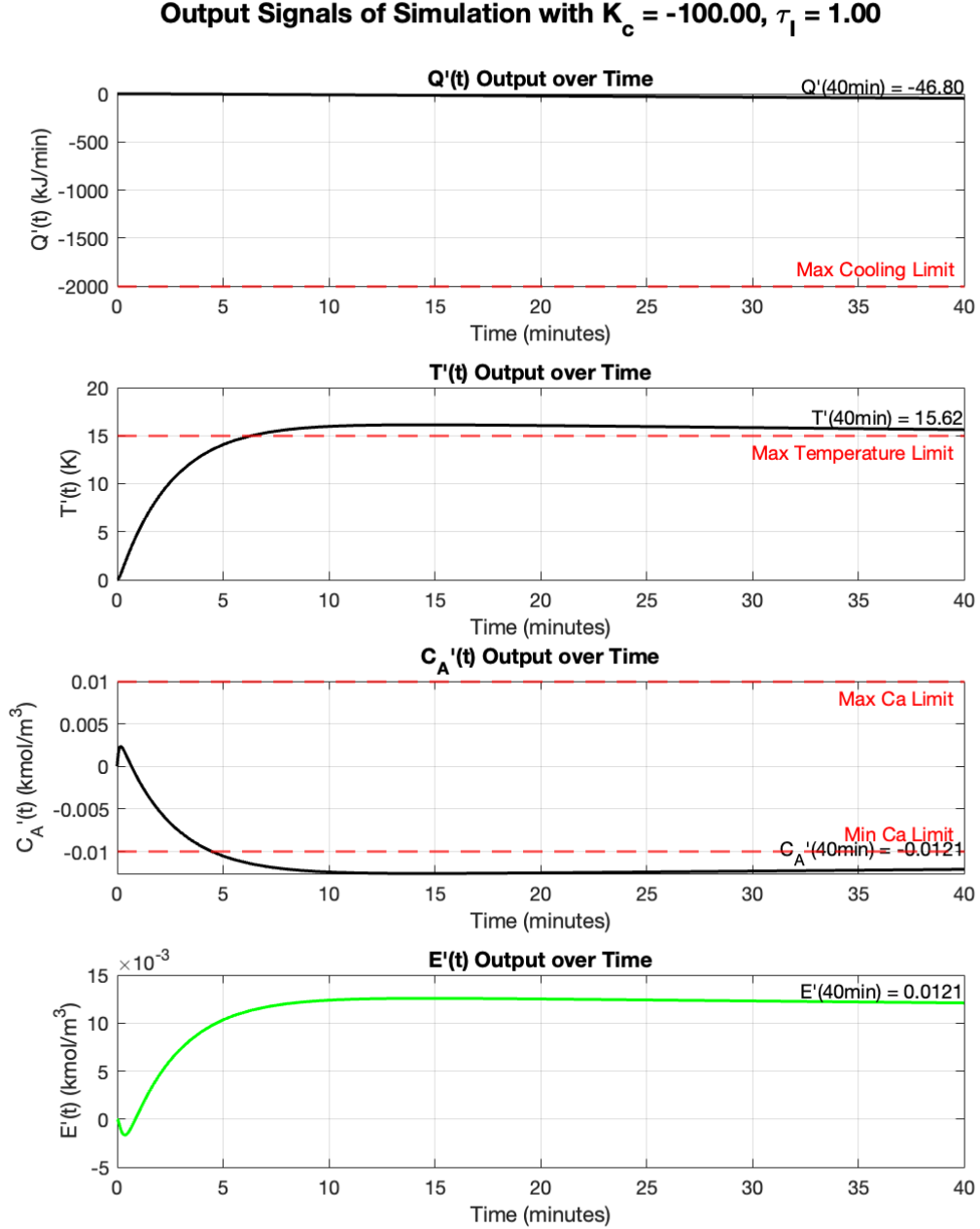


Figure 22: System response with $K_c = -100.00$, $\tau_I = 1.00$

Test Case 3: $K_c = -100.00$, $\tau_I = 0.10$

With a reduced τ_I , the system becomes more responsive. As shown in Figure 23, both $C'_A(t)$ and $T'(t)$ begin returning toward zero, but still overshoot the design limits early in the simulation. This indicates the controller is not yet aggressive enough to fully compensate for the disturbance. Therefore, we further increase K_c by another factor of 10.

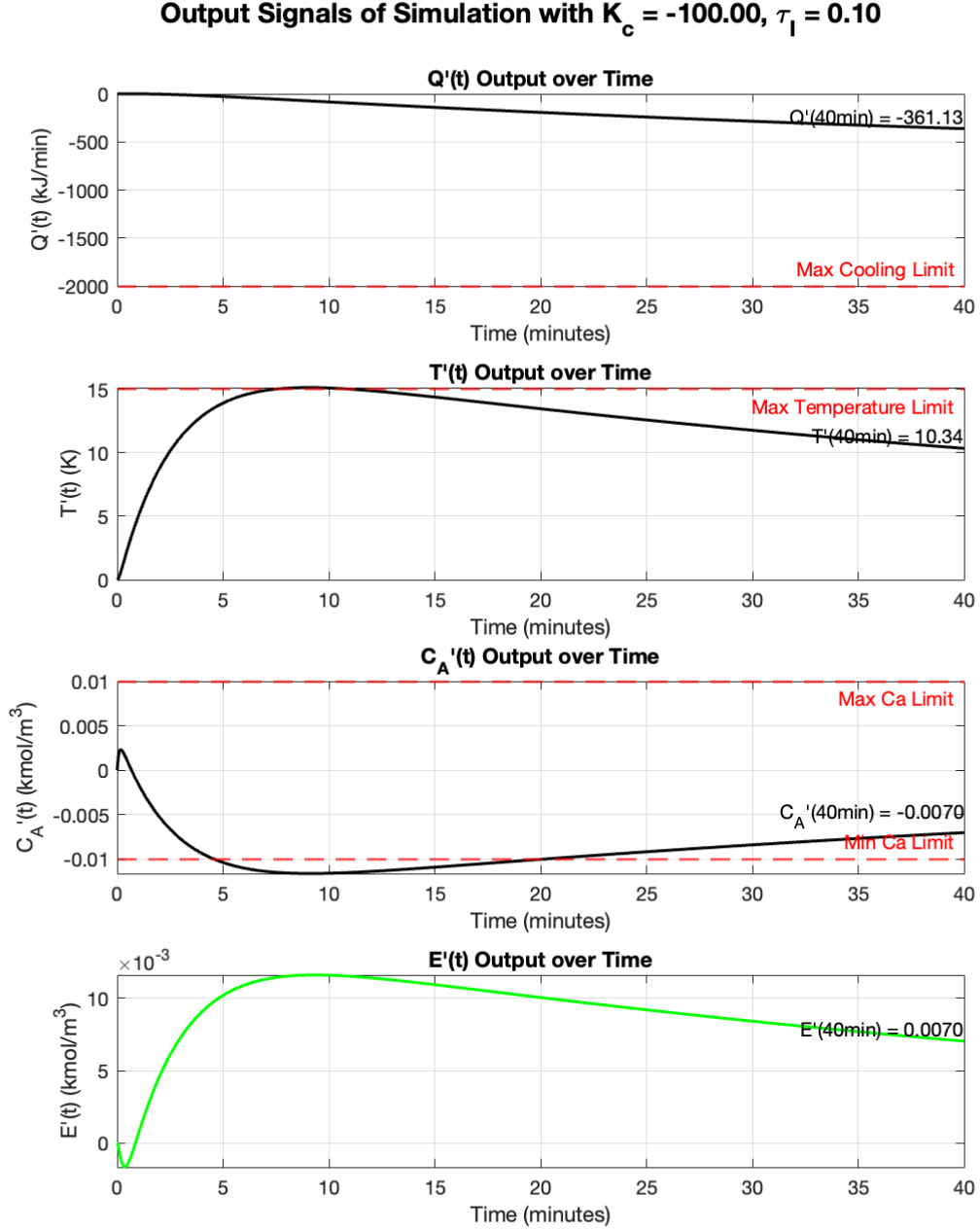


Figure 23: System response with $K_c = -100.00$, $\tau_I = 0.10$

Test Case 4: $K_c = -1000.00$, $\tau_I = 0.10$

Figure 24 shows that with this configuration, all design objectives are successfully met. The concentration deviation $C'_A(t)$ stays within the ± 0.01 bounds, the temperature remains under 15 K after the initial peak, and $Q'(t)$ does not exceed the minimum limit of -2000 kJ/min. Not only that but $C'_A(t)$ returns to 0 at the end of the 40 mins. Additionally, the error $E'(t)$ converges back to zero. This configuration is selected as the final design.

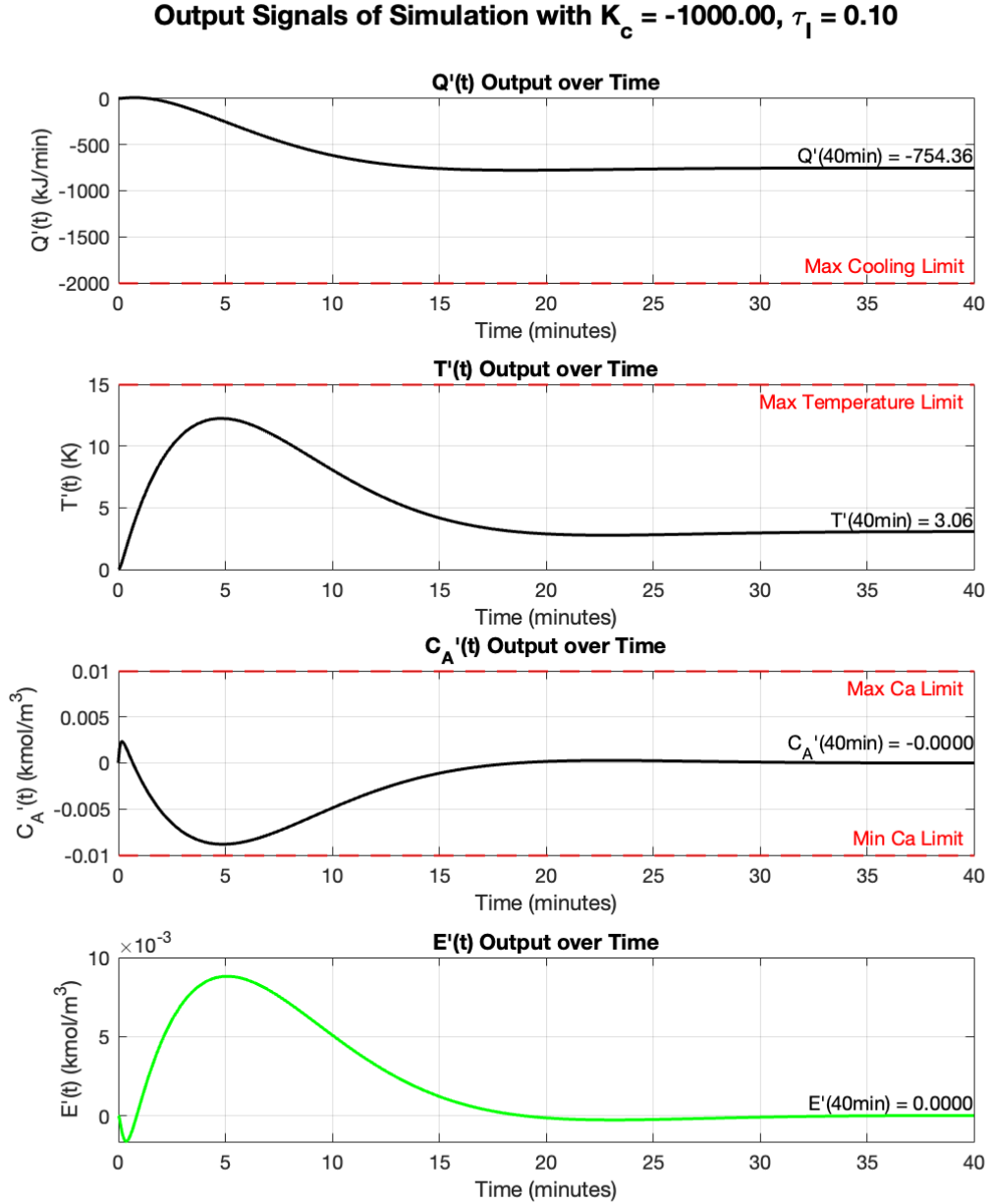


Figure 24: System response with $K_c = -1000.00$, $\tau_I = 0.10$